World Academy of Science, Engineering and Technology
International Journal of Electronics and Communication Engineering
Vol:12, No:9, 2018

Parameter Estimation of Diode Circuit Using Extended Kalman Filter

Amit Kumar Gautam, Sudipta Majumdar

Abstract—This paper presents parameter estimation of a single-phase rectifier using extended Kalman filter (EKF). The state space model has been obtained using Kirchhoff's current law (KCL) and Kirchhoff's voltage law (KVL). The capacitor voltage and diode current of the circuit have been estimated using EKF. Simulation results validate the better accuracy of the proposed method as compared to the least mean square method (LMS). Further, EKF has the advantage that it can be used for nonlinear systems.

Keywords—Extended Kalman filter, parameter estimation, single phase rectifier, state space modelling.

I. Introduction

SINGLE phase rectifier has been used in many applications such as variable speed motor drive [1]-[3], split capacitor full bridge rectifier [4], single phase full-bridge resonant circuit [5] etc.

Parameter estimation of different diode circuits have been proposed in literature. In [6], Yeh *et al*. proposed a method that uses both the simplified swarm optimization and Nelder-Mead simplex algorithm for parameter identification of photovoltaic system. This method has the advantage of fast and accurate parameter identification. It also performs well in terms of run time and standard deviation of fitness value. In [7], Jadli *et al*. presented mathematical model of solar photovoltaic (PV) cell for estimation of electrical parameters such as diode dark saturation current, diode ideality factor etc. which vary with environmental conditions. Further, they used the proposed model together with analytical method and simplified annealing method to present a new estimation method. They compared with other methods to reveal the better performance of the proposed method. In [8], Zadeh *et al*. proposed modelling of PV arrays and estimation of maximum power point (MPP) by measuring the voltage and current at three points near the MPP. The advantage of the method is that there is no oscillation near the MPP. Also, it has the advantage of less computational complexity, small run time and decrease in the I-V characteristic estimation loss. Xu *et al*. [9] used density of nonradiated recombination defects to estimate the lifetime in light emitting diode (LED) chip.

Batzelis *et al*. [10] proposed a method for MPP estimation by fitting a curve on voltage and current measurements. This method has the advantage of good accuracy and noise robustness during fast changing environmental conditions. Attivissimo *et al*. [11] estimated the series and shunt resistances of a PV cell using Levenberg Marquarclt algorithm based optimization method. They used seven parameter model of a PV cell. In [12], Kim *et al*. proposed a method for lifetime estimation of organic LED (OLED) that uses bivariate acceleration model and a statistical method that considers uncertainties. They also used likelihood ratio based method to validate the proposed method. Dusmez *et al*. [13] proposed method for lifetime estimation of power metal oxide semiconductor field effect transistor (MOSFET) and insulated gate bipolar transistors. The lifetime is estimated by modelling the gate threshold voltage. The least square method has been used for model parameter estimation. Chen *et al*. [14] proposed electrical measurement procedure for estimation of carrier concentration of LED. Savuskan *et al*. [15] used semi empirical and analytical models to estimate the photon detection efficiency nonuniformity of avalanche diode.

This paper is organized as follows. Section II presents LMS algorithm. Section III introduces EKF algorithm. The state space modelling of single phase full wave rectifier circuit has been derived in Section IV. Section V presents simulation results. Finally, Section VI presents conclusions.

A. K. Gautam and S. Majumdar are with Electronics and Communication Engineering Department, DTU, New Delhi 110042, India (e-mail: amitgautam.cicdu@gmail.com, korsudipta@rediffmail.com).

II. Least Mean Square Algorithm

LMS is an adaptive filter which is used for system identification. The LMS [16]-[22] minimizes the instantaneous error squared. It requires minimum storage as it only requires to store the filter weights.In this search algorithm, the gradient vector computation is simplified by appropriate modification of the objective function. It is broadly used for various applications as it has the advantage of low computational cost and implementation simplicity.

Let $x(n)$ is the input signal to the filter, $y(n)$ is the output signal and $d(n)$ is the desired signal. $y(n)$ depends on $\bar{u}(n)$ such as:

$$y(n) = \bar{u}(n)^T \bar{w}(n) \quad (1)$$

where $\bar{w}(n)$ is the weighted coefficient such as $\bar{w}(n) = [w_1(n), w_2(n)...w_N(n)]^T$ and $\bar{u}(n) = [x_1(n), x_2(n)...x_N(n)]^T$.

The LMS algorithm find the filter coefficients by minimizing the cost function. The cost function is

$$J(n) = \frac{1}{2}E\{e(n)\}^2 \quad (2)$$

The adaptive filter coefficient is updated using the following operations:

1) Calculation of adaptive filter output signal $y(n)$.
2) Calculation of the error signal

$$e(n) = d(n) - y(n) \tag{3}$$

3) Update the filter coefficient by using following expression:

$$\bar{w}(n+1) = \bar{w}(n) + \mu e(n)\bar{u}(n) \tag{4}$$

where μ is the step size of the adaptive filter, $\bar{w}(n)$ is the filter coefficient vector. $\bar{u}(n)$ is the filter input vector.

III. EKF Algorithm

EKF is broadly used for estimation purpose in various applications [23]-[25]. It uses linearized model of the nonlinear system to implement Kalman filtering. The linearization process uses the partial derivative or Jacobian matrices of nonlinear function of the model. Using a priori and posteriori error covariance, the estimation process is defined in terms of the linearized observation model. The algorithm starts with initialization of mean value of the state vector and covariance matrix.

A nonlinear discrete time system can be expressed by its difference equations as:

$$x_k = f(x_{k-1}, u_{k-1}) + w_{k-1} \tag{5}$$

$$y_k = h(x_k, u_k) + v_k \tag{6}$$

Equations (5) and (6) are represented in terms of nonlinear state model and measurement model respectively. where $f(.)$ and $h(.)$ are nonlinear functions of process and measurement model. w_k and v_k are the Gaussian noise disturbance with zero mean with covariance matrix Q_k and R_k respectively. Consider all assumptions as below:
$E[w_k] = 0$, $E[w_k, w_k^T] = Q_k$, $E[w_k, w_j^T] = 0 \forall k \neq j$, $E[w_k, x_0^T] = 0 \forall K$, $E[v_k] = 0$, $E[v_k, v_k^T] = R_k$, $E[v_k, v_j^T] = 0 \forall k \neq j$, $E[v_k, x_0^T] = 0 \forall k$, $E[w_k, v_j^T] = 0 \forall k \& j$.

The steps involved for EKF algorithm are as follows:

Step 1. State initialization: Assume the mean μ_0 and covariance P_0 of the states as below:

$$\hat{x}_0 = \mu_0 = E[x_0] \tag{7}$$

$$P_0 = E[(x_0 - \hat{x}_0)(x_0 - \hat{x}_0)^T] \tag{8}$$

State estimation at time $k-1$

$$\hat{x}_{k-1|k-1} = E[(x_{k-1}|y_{k-1})] \tag{9}$$

Step 2. State prediction: The predicted value of x_k is given as

$$\hat{x}_{k|k-1} = E[(x_k|y_{k-1})] \tag{10}$$

Taylor's series expansions are applied to linearized the nonlinear model of (5).

$$x_k = f_{k-1}(\hat{x}_{k-1|k-1}, 0) + F_{k-1}(\tilde{x}_{k-1}) + \Delta f(\tilde{x}_{k-1}^2) \tag{11}$$

where $\Delta f(\tilde{x}_{k-1}^2)$ is the higher order terms of Taylor's series expansion. F_k is the Jacobian matrix and can be expressed as

$$F_k = \begin{bmatrix} \frac{df_1}{dx_1} & \frac{df_1}{dx_2} & \frac{df_1}{dx_3} & \cdots & \frac{df_1}{dx_n} \\ \vdots & \vdots & \vdots & \ddots & \vdots \\ \frac{df_p}{dx_1} & \frac{df_p}{dx_2} & \frac{df_p}{dx_3} & \cdots & \frac{df_p}{dx_n} \end{bmatrix}$$

where $f(x) = (f_1(x), f_2(x), ...f_p(x))^T$ and $x_k = (x_1, x_2, ...x_p)^T$. substituting the value of x_k from (11) into (10), we get

$$\hat{x}_{k|k-1} = f(\hat{x}_{k-1|k-1}, u_k) \tag{12}$$

Covariance error is defined as

$$P_{k|k-1} = E[e_k e_k^T] \tag{13}$$

where $e_k = x_k - \hat{x}_k$. Solving (13), we obtain the predicted covariance error as:

$$P_{k|k-1} = F_k P_{k-1|k-1} {F_k}^T + Q_k \tag{14}$$

Step 3. Measurement prediction: We have predicted value $\hat{x}_{k|k-1}$ with covariance $P_{k|k-1}$ and measurement y_k with covariance R_k. The objective is to find best estimation $\hat{x}_{k|k}$ in terms of least square sense. Putting the value of from (11) into (6), we calculate the predicted measurement $\hat{y}_{k|k-1}$ as

$$\hat{y}_{k|k-1} = h(\hat{x}_{k|k-1}) \tag{15}$$

Observation error can be defined as

$$Z_{k|k-1} = y_k - \hat{y}_{k|k-1} \tag{16}$$

By using (14), observation error covariance can be calculated as

$$S_k = E[Z_{k|k-1}(Z_{k|k-1})^T] = H_k P_{k|k-1} {H_k}^T + R_k \tag{17}$$

where

$$H_k = \begin{bmatrix} \frac{dh_1}{dx_1} & \frac{dh_1}{dx_2} & \frac{dh_1}{dx_3} & \cdots & \frac{dh_1}{dx_n} \\ \vdots & \vdots & \vdots & \ddots & \vdots \\ \frac{dh_p}{dx_1} & \frac{dh_p}{dx_2} & \frac{dh_p}{dx_3} & \cdots & \frac{dh_p}{dx_n} \end{bmatrix}$$

where $h(x) = (h_1(x), h_2(x), ...h_p(x))^T$ and $x = (x_1, x_2, ...x_p)^T$.

Step 4. Measurement update: The state estimation is calculated as

$$\hat{x}_{k|k} = \hat{x}_{k|k-1} + K_K(y_k - h(\hat{x}_{k|k-1})) \tag{18}$$

The predicted covariance is

$$\begin{aligned} P_{k|k} &= E[e_{k|k} e_{k|k}^T | y_k] \\ &= P_{k|k-1} - K_K(H_k P_{k|k-1} H_k^{-1} + R_k) {K_K}^T \end{aligned} \tag{19}$$

where Kalman gain is

$$K_K = P_{k|k-1} H_k^T (H_k P_{k|k-1} H_k^{-1} + R_k)^{-1} \tag{20}$$

Table I summarizes the EKF steps.

IV. State Space Model for Single Phase Rectifier Circuit

Fig. 1 shows single-phase full wave rectifier circuit. The input voltage is $v_i(t)$. The circuit consists of inductor L_s and resistor R_s. The capacitor C is used at the output, which is in parallel with the load resistance R_L. We assumed that D_1 to D_4 are identical diodes with voltage drop equal to v_D. $i_D(t)$ and $v_c(t)$ are the diode current and capacitor voltage respectively.

TABLE I
ALGORITHM OF EKF

Algorithm 1: Extended Kalman Filter

1. Initialization step:
Initialize $\hat{x}_{k-1|k-1}$, $P_{k-1|k-1}$, Q_{k-1} and R_k

2. State prediction:
Compute matrices F_k as:
$F_k = \frac{\partial f_i(x,u_k)}{\partial x}|_{x=\hat{x}_i}$
Compute state $\hat{x}_{k|k-1}$ as:
$\hat{x}_{k|k-1} = f_{k-1}(\hat{x}_{k-1|k-1}, 0)$
Compute predicted covariance of error:
$P_{k|k-1} = F_k P_{k-1|k-1} F_k^T + Q_{k-1}$

3.Measurement update:
Compute matrices H_k as:
$H_k = \frac{\partial h_i(x,u_k)}{\partial x}|_{x=\hat{x}_i}$
Compute the Kalman gain as:
$K_k = P_{k|k-1} H_k^T (H_k P_{k|k-1} H_k^T + R_k)^{-1}$
Update the state estimation:
$\hat{x}_{k|k} = \hat{x}_{k|k-1} + K_k(y_k - h_k(\hat{x}_{k|k-1}))$
Compute covariance error matrix:
$P_{k|k} = (I - K_k H_k) P_{k|k-1}$

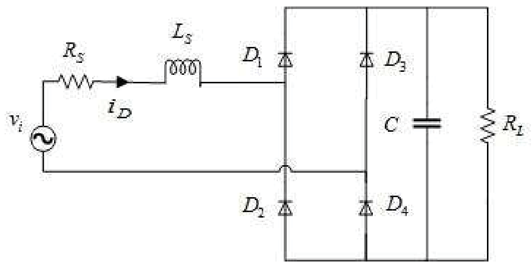

Fig. 1 Circuit diagram of single-phase full wave rectifier

The circuit equations of rectifier have been obtained using Kirchhoff's voltage and current laws. They are:

$$C\frac{d}{dt}v_c(t) + \frac{v_c(t)}{R_L} = i_D(t) \tag{21}$$

$$v_i(t) = R_S i_D(t) + L_S \frac{d}{dt} i_D(t) + 2v_D + v_c(t) \tag{22}$$

where $i_D(t) = I_0(e^{v_D/v_T} - 1)$.

Representing (21) and (22) in terms of state equations, we have

$$\frac{d}{dt}v_c(t) = -\frac{1}{R_L C}v_c(t) + \frac{1}{C}i_D(t) \tag{23}$$

$$\frac{d}{dt}i_D(t) = -\frac{1}{L_S}v_c(t) - \frac{(R_S + 2V_T/I_0)}{L_S}i_D(t) + \frac{1}{L_S}v_i(t) \tag{24}$$

Here, V_T and I_0 denote the thermal voltage and reverse saturation current of diode respectively. Similarly, representing the dynamic equations (23) and (24) as state space equations, we have

$$\frac{d}{dt}x(t) = Fx(t) + Bv_i(t) \tag{25}$$

where $x(t)$ is the state vector consisting of two states $v_c(t)$ and $i_D(t)$ respectively. The state transition matrix F and input vector B are:

$$F = \begin{bmatrix} -\frac{1}{R_L C} & \frac{1}{C} \\ -\frac{1}{L_S} & -\frac{(R_S+2V_T/I_0)}{L_S} \end{bmatrix}$$

and

$$B = \begin{bmatrix} 0 & \frac{1}{L_S} \end{bmatrix}^T \tag{26}$$

The state space model is given as:

$$\frac{d}{dt}\begin{bmatrix} v_c(t) \\ i_D(t) \end{bmatrix} = \begin{bmatrix} -\frac{1}{R_L C} & \frac{1}{C} \\ -\frac{1}{L_S} & -\frac{(R_S+2V_T/I_0)}{L_S} \end{bmatrix} \begin{bmatrix} v_c(t) \\ i_D(t) \end{bmatrix} + \begin{bmatrix} 0 \\ \frac{1}{L_S} \end{bmatrix} v_i(t) \tag{27}$$

The measurement model is:

$$y(t) = Cx(t) \tag{28}$$

where

$$C = \begin{bmatrix} 1 & 0 \end{bmatrix}$$

The discrete form of (27) can be obtained using Euler-Maruyama method. Substituting $t = kT_s$, where k is a positive integer value and T_s is sampling time. In general, the discrete time state space equations can be written as:

$$x_{k+1} = F_d x_k + B_d v_{i_k} + w_k \tag{29}$$

$$y_k = C_d x_k + v_k \tag{30}$$

The matrices F_d, B_d and C_d are

$$F_d = \begin{bmatrix} 1 - \frac{T_s}{R_L C} & \frac{T_s}{C} \\ -\frac{T_s}{L_S} & 1 - \frac{T_s(R_S+2V_T/I_0)}{L_S} \end{bmatrix}$$

$$B_d = \begin{bmatrix} 0 \\ \frac{T_s}{L_S} \end{bmatrix}$$

and

$$C_d = \begin{bmatrix} 1 \\ 0 \end{bmatrix}^T \tag{31}$$

w_k and v_k are the process noise and measurement noise respectively which are zero mean Gaussian noise.

V. Simulation Results

The parameters of rectifier circuit have been estimated in MATLAB using EKF and compared with LMS estimation method. Sinusoidal input of 10 volts and 50 KHz frequency has been used as shown in Fig. 2. The system noise and measurement noise used are white Gaussian noise of zero mean with 0.5 and 0.1 variance respectively. The PSPICE simulated values have been considered as the actual value. Simulations have been performed using noiseless input signal and noisy input signal. Figs. 3-12 show the comparison of estimated capacitor voltage and diode current using EKF and LMS with PSPICE simulations. Table II and Table III compare the root mean square error (RMSE) and signal to noise ratio (SNR) of EKF and LMS method for capacitor voltage and diode current respectively.

TABLE II
COMPARISON OF CAPACITOR VOLTAGE (v_C) ESTIMATION USING DIFFERENT METHODS

Input signal	Parameter	LMS method	EKF method
Noiseless input	SNR(dB) RMSE	0.42 1.24	1.07 0.86
Noisy input signal with mean 0 and variance 0.1	SNR(dB) RMSE	0.40 1.50	1.01 0.96
Noisy input signal with mean 0 and variance 0.5	SNR(dB) RMSE	0.35 2.10	1.00 1.01
Noisy input signal with mean 0 and variance 1.0	SNR(dB) RMSE	0.26 2.15	0.90 1.02
Noisy input signal with mean 0 and variance 2.0	SNR(dB) RMSE	0.10 3.17	0.76 2.42

TABLE III
COMPARISON OF DIODE CURRENT (i_D) ESTIMATION USING DIFFERENT METHODS

Input signal	Parameter	LMS method	EKF method
Noiseless input	SNR(dB) RMSE	0.258 0.69	1.290 0.3359
Noisy input signal with mean 0 and variance 0.1	SNR(dB) RMSE	0.20 1.40	1.05 0.66
Noisy input signal with mean 0 and variance 0.5	SNR(dB) RMSE	0.16 2.45	1.01 1.56
Noisy input signal with mean 0 and variance 1.0	SNR(dB) RMSE	0.10 2.55	1.0 1.82
Noisy input signal with mean 0 and variance 2.0	SNR(dB) RMSE	0.054 2.95	0.87 2.56

$$RMSE = \sqrt{\frac{\sum_{i=1}^{n} (\widehat{y}_i - y_i)^2}{n}} \tag{32}$$

$$SNR = \sqrt{\frac{\sum_{i=1}^{n} (\widehat{y}_i)^2}{\sum_{i=1}^{n} (\widehat{y}_i - y_i)^2}} \tag{33}$$

where $\hat{y}$ is the estimated value, y is the actual value and n is the number of samples.

VI. CONCLUSIONS

The parameter estimation of a single-phase rectifier using EKF is presented in this paper. The voltage across the capacitor and diode current have been estimated using EKF method and compared with LMS estimation method. Simulation results show the better SNR value for EKF as compared to LMS method. Also, EKF has smaller value of RMSE as compared to LMS estimation method. Further, EKF has the advantage that it can be used for nonlinear systems.

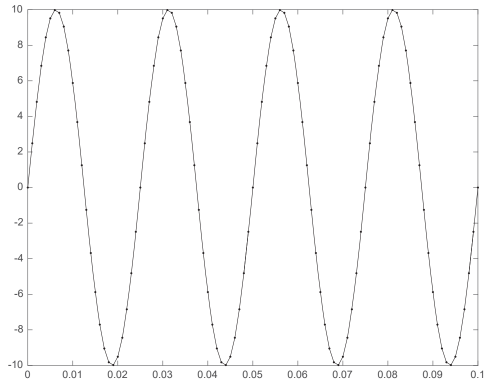

Fig. 2 Input sinusoidal signal.

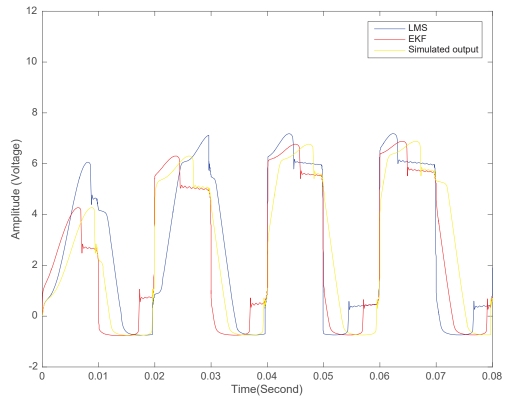

Fig. 3 Estimated voltage using EKF and LMS method for noiseless input signal

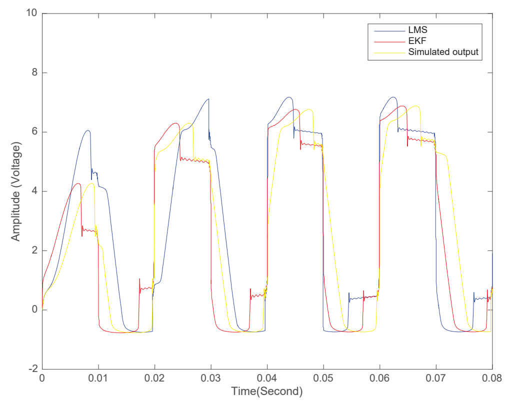

Fig. 4 Estimated voltage using EKF and LMS method for noisy input signal with zero mean and variance 0.1

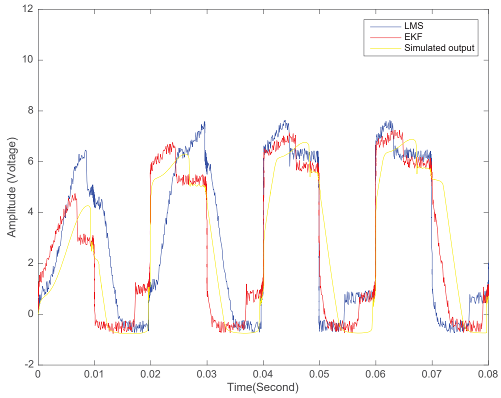

Fig. 5 Estimated voltage using EKF and LMS method for noisy input signal with zero mean and variance 0.5

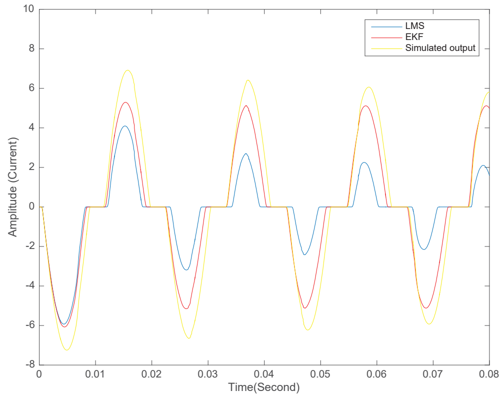

Fig. 8 Estimated current using EKF and LMS method for noiseless input signal

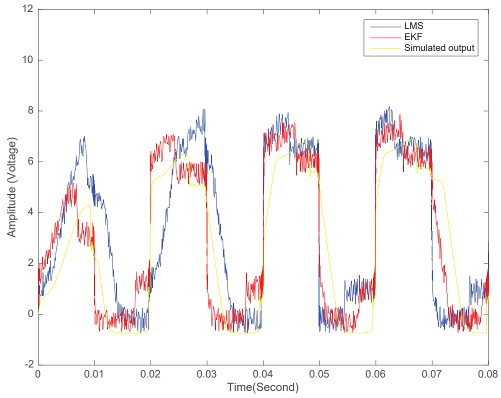

Fig. 6 Estimated voltage using EKF and LMS method for noisy input signal with zero mean and variance 1.0

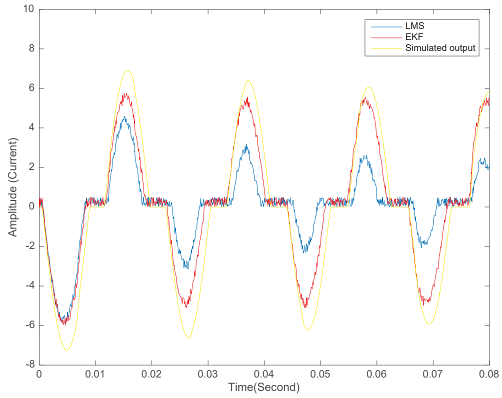

Fig. 9 Estimated current using EKF and LMS method for noisy input signal with zero mean and variance 0.1

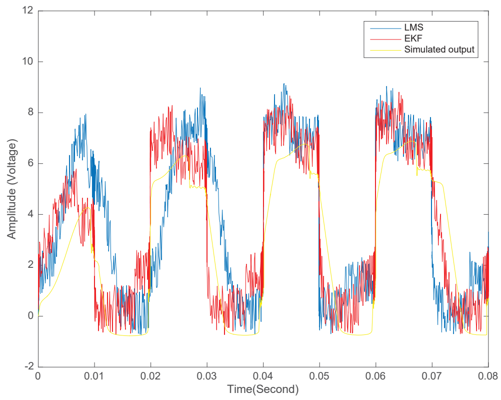

Fig. 7 Estimated voltage using EKF and LMS method for noisy input signal with zero mean and variance 2.0

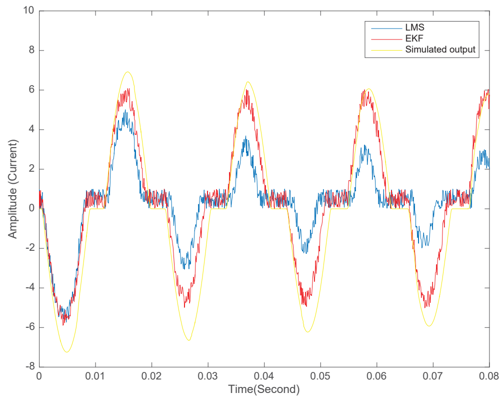

Fig. 10 Estimated current using EKF and LMS method for noisy input signal with zero mean and variance 0.5

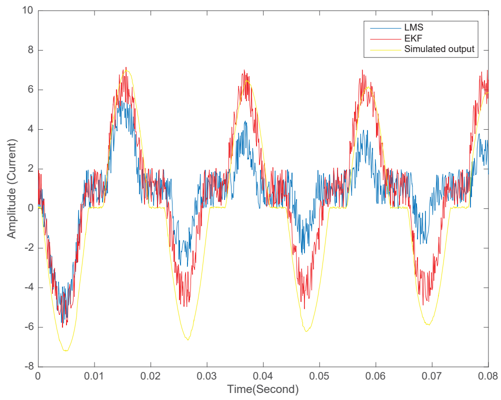

Fig. 11 Estimated current using EKF and LMS method for noisy input signal with zero mean and variance 1.0

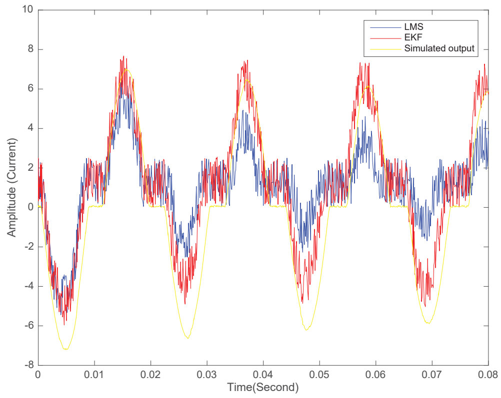

Fig. 12 Estimated current using EKF and LMS method for noisy input signal with zero mean and variance 2.0

ACKNOWLEDGMENT

First author thanks UGC, India.

REFERENCES

[1] Y. Son and J.I. Ha, "Discontinuous grid current control of motor drive system with single-phase diode rectifier and small DC-link capacitor," *IEEE Transactions on Power Electronics*, vol. 32, no. 2, pp. 1324-1334, 2017.

[2] Y. Son and J. I. Ha, "Direct power control of a three-phase inverter for grid input current shaping of a single-phase diode rectifier with a small DC-link capacitor," *IEEE Transactions on Power Electronics*, vol. 30, no. 7, pp. 3794-3803, 2015.

[3] W. J. Lee, Y. Son and J. I. Ha, "Single-phase active power filtering method using diode-rectifier-fed motor drive," *IEEE Transactions on Industry Applications*, vol. 51, no. 3, pp. 2227-2236, 2015.

[4] S. Gupta, V. Nimesh and V. John, "Diode bridge rectifier with improved power quality using capacitive network," *IEEE International Conference on Power Electronics, Drives and Energy Systems (PEDES)*, pp. 1-6, 2016.

[5] P. Wang, C. Liu and L. Guo, "Modeling and simulation of full-bridge series resonant converter based on generalized state space averaging," *In Applied Mechanics and Materials*, vol. 347, pp. 1828-1832, 2013.

[6] W. C. Yeh, C. L. Huang, P. Lin, Z. Chen, Y. Jiang and B. Sun, "Simplex simplified swarm optimisation for the efficient optimisation of parameter identification for solar cell models," *IET Renewable Power Generation*, vol. 12, no. 1, pp. 45-51, 2017.

[7] U. Jadli, P. Thakur and R. D. Shukla. "A new parameter estimation method of solar photovoltaic," *IEEE Journal of Photovoltaics*, vol. 8, no. 1, pp. 239-247, 2018.

[8] M. J. Zadeh and S. H. Fathi, "A new approach for photovoltaic arrays modeling and maximum power point estimation in real operating conditions," *IEEE Transactions on Industrial Electronics*, vol. 64, no. 12, pp. 9334-9343, 2017.

[9] L. W. Xu and K. Y. Qian, "A fast method for lifetime estimation of blue light-emitting diode chips based on nonradiative recombination defects," *IEEE Photonics Journal*, vol. 9, no. 4, pp. 1-9, 2017.

[10] E. I. Batzelis, G. E. Kampitsis and S. A. Papathanassiou, "Power reserves control for PV systems with real-time MPP estimation via curve fitting," *IEEE Transactions on Sustainable Energy*, vol. 8, no. 3, pp. 1269-1280, 2017.

[11] F. Attivissimo, A. Di Nisio, M. Savino and M. Spadavecchia, "Uncertainty analysis in photovoltaic cell parameter estimation," *IEEE Transactions on Instrumentation and Measurement*, vol. 61, no. 5, pp. 1334-1342, 2012.

[12] D. W. Kim, H. Oh, B. D. Youn and D. Kwon, "Bivariate lifetime model for organic light-emitting diodes," *IEEE Transactions on Industrial Electronics*, vol. 64, no. 3, pp. 2325-2334, 2017.

[13] S. Dusmez, S. H. Ali, M. Heydarzadeh, A. S. Kamath, H. Duran and B. Akin, "Aging precursor identification and lifetime estimation for thermally aged discrete package silicon power switches," *IEEE Transactions on Industry Applications*, vol. 53, no. 1, pp. 251-60, 2017.

[14] H. T. Chen, X. F. Zhou, J. Y. Cai and S. Lin, "Estimation carrier concentration of light-emitting diode via electricalthermal characteristics," *IEEE Transactions on Electron Devices*, vol. 62, no. 7, pp. 2257-2262, 2015.

[15] V. Savuskan, I. Brouk, M. Javitt, Y. Nemirovsky, "An estimation of single photon avalanche diode (SPAD) photon detection efficiency (PDE) nonuniformity," *IEEE Sensors Journal*, vol. 13, no. 5, pp. 1637-1640, 2013.

[16] W. A Ali, D. A. Mohamed and A. H. Hassan, "Performance analysis of least mean square sample matrix inversion algorithm for smart antenna system," *In Antennas and Propagation Conference (LAPC) IEEE*, pp. 624-629, 2013.

[17] D. Z. Feng, Z. Bao and L. C. Jiao, "Total least mean squares algorithm," *IEEE Transactions on Signal Processing*, vol. 46, no. 8, pp. 2122-2130, 1998.

[18] A. K. Pradhan, A. Routray and A. Basak, "Power system frequency estimation using least mean square technique" *IEEE transactions on power delivery*, vol. 20, no. 3, pp. 1812-1816, 2005.

[19] W. Edmonson, J. Principe, K. Srinivasan and C. Wang, "A global least mean square algorithm for adaptive IIR filtering," *IEEE Transactions on Circuits and Systems II: Analog and Digital Signal Processing*, vol. 45, no. 3, pp. 379-384, 1998.

[20] I. Lakkis and D. McLernon, "Least mean squares algorithm for fractionally spaced blind channel estimation," *IEE Proceedings-Vision, Image and Signal Processing*, vol. 146, no. 4, pp. 181-184, 1999.

[21] A. Flammini, D. Marioli, E. Sisinni and A. Taroni, "Least mean square method for LVDT signal processing," *IEEE Transactions on Instrumentation and Measurement*, vol. 56, no. 6, pp. 2294-2300, 2007.

[22] A. Tarighat and A. H. Sayed, "Least mean-phase adaptive filters with application to communications systems," *IEEE Signal Processing Letters*, vol. 11, no. 2, pp. 220-223, 2004.

[23] A. K. Gautam and S. Majumdar, "Parameter estimation of RC circuits using extended Kalman filter," *International Journal of Advanced in Management, Technology and Engineering Sciences*, vol. 8, no. 1, pp. 83-91, 2018.

[24] R. Bansal and S. Majumdar, "Implementation of extended Kalman filter on stochastic model of LPF," *International Journal of Advanced in Management, Technology and Engineering Sciences*, vol. 7, no. 12, 2017.

[25] P. Stano, Z. Lendek, J. Braaksma, R. Babuska, C. de Keizer and J. Arnold. "Parametric bayesian filters for nonlinear stochastic dynamical systems: a survey," *IEEE transactions on cybernetics*, vol. 43, no. 6, pp. 1607-1624, 2013.